BioTechniques

ISSN: 0736-6205 (Print) 1940-9818 (Online) Journal homepage: www.tandfonline.com/journals/ibtn20

Tumor Cell Invasion into Matrigel: Optimized Protocol for RNA Extraction

Roberta Ferretti, Antonella Baldassarre, Emmanuel de Billy, Angel M Carcaboso, Andrew Moore, Andrea Carai, Angela Mastronuzzi, Andrea Masotti & Maria Vinci

To cite this article: Roberta Ferretti, Antonella Baldassarre, Emmanuel de Billy, Angel M Carcaboso, Andrew Moore, Andrea Carai, Angela Mastronuzzi, Andrea Masotti & Maria Vinci (2021) Tumor Cell Invasion into Matrigel: Optimized Protocol for RNA Extraction, BioTechniques, 70:6, 327-335, DOI: 10.2144/btn-2021-0001

To link to this article: https://doi.org/10.2144/btn-2021-0001

Reports

BioTechniques

Tumor cell invasion into Matrigel: optimized protocol for RNA extraction

Roberta Ferretti[1], Antonella Baldassarre[2], Emmanuel de Billy[1], Angel M Carcaboso[3], Andrew Moore[4,5], Andrea Carai[6], Angela Mastronuzzi[7], Andrea Masotti[2] & Maria Vinci*,[1]

*[1]Department of Onco-haematology, Gene & Cell Therapy, Bambino Gesù Children's Hospital-IRCCS, Rome, 00146, Italy; [2]Multifactorial & Complex Phenotypes Research Area, Bambino Gesù Children's Hospital-IRCCS, Rome, 00146, Italy; [3]Developmental Tumor Biology Laboratory, Hospital Sant Joan de Déu, Barcelona, 08004, Spain; [4]Oncology Service, Queensland Children's Hospital, Brisbane, 4101, Australia; [5]Child Health Research Centre, The University of Queensland, Brisbane, 4101, Australia; [6]Oncological Neurosurgery Unit, Department of Neuroscience & Neurorehabilitation, Bambino Gesù Children's Hospital-IRCCS, Rome, 00165, Italy; [7]Neuro-oncology Unit, Department of Onco-hematology, Gene & Cell Therapy, Bambino Gesù Children's Hospital-IRCCS, Rome, 00165, Italy; *Author for correspondence: Tel.: +39 0668592657; maria.vinci@opbg.net*

BioTechniques 70: 327–335 (June 2021) 10.2144/btn-2021-0001

First draft submitted: 5 January 2021; Accepted for publication: 14 April 2021; Published online: 10 May 2021

ABSTRACT

3D models are increasingly used to study mechanisms driving tumor progression and mimicking *in vitro* processes such as invasion and migration. However, there is a need to establish more protocols based on 3D culture systems that allow for downstream molecular biology investigations. **Materials & methods:** Here we present a method for optimal RNA extraction from highly aggressive primary glioma cells invading into Matrigel. The method has been established by comparing previously reported protocols, available commercial kits and optimizing specific steps for matrix dissociation, RNA separation and purification. **Results and conclusion:** The protocol allows RNA extraction from cells embedded into Matrigel, with optimal yield, purity and integrity suitable for subsequent sequencing analysis of both high and low molecular weight RNA.

METHOD SUMMARY

An optimized method for RNA extraction from highly invasive glioma cells embedded into Matrigel was achieved by using TRIzol, used for matrix dissociation, cell lysis and RNA separation, in combination with a specific commercial kit used to perform the DNAse treatment and optimal RNA purification on column. The method ensures optimal yield, good purity and integrity for analysis of high and low molecular weight RNA molecules.

KEYWORDS:

3D ● invasion ● Matrigel ● miRNA ● mRNA ● RNA

Several findings in oncogenesis and stem cell differentiation elucidate the disparities in cell behavior between 2D and 3D cultures [1–4]. In 2D, cells are removed from their physiological context and lack cell–cell and cell–matrix interactions, impacting not only on cell shape and membrane composition but on the whole cell functionality [1,3–5]. The 2D/3D dissimilarity is profound for processes in which cells 'move' in the tissue, such as cell migration and invasion (crucial during embryogenesis), development and tissue regeneration, as well as tumor progression [3,4,6].

For these reasons, during the last few decades we have seen a progressive increase in the use of 3D models in replacement of the 2D cell monolayers in different fields of research, including bioengineering, oncology and drug discovery [1,5–8]. 3D models combine the versatility and reproducibility of an *in vitro* system with a proper veracity, without the variability, time and costs typical of *in vivo* procedures [1,9]. The continuous development of new cell culture methods gave rise to a series of 3D models differing for cell types used, their origins and differentiation states [9–13]. Spheroids, among the most common 3D culture models, are multicellular spheroidal aggregates growing in suspension, in which cells establish cell–cell interactions and are exposed to gradients of oxygen and nutrients from the surface to the core [12,14]. Although they reproduce the pathophysiological complexity of tumor tissues (albeit only at a basic level), they are versatile, simple and suitable for high-throughput studies [12,14–16].

The development of 3D technologies has progressed in parallel with the advancements of new biomaterials mimicking the structural and functional composition of extracellular matrices and basal membranes of the cell niches [3,5,6,11,17,18]. Biomaterials can be purely natural (matrix-based systems), synthetic (scaffolds – porous cellular solids), or hybrids [3,5,11,18]. The most common include extracellular matrix components such as laminin, collagen, fibrin and hyaluronic acid, used alone or mixed, forming hydrogels [3,5,11,18]. One of the most used, Matrigel, is a basement membrane matrix derived from Engelbreth–Holm–Swarm mouse sarcoma and is particularly suitable for tumor growth, invasion and migration studies [14,16,19–21].

Table 1. Short tandem repeat analysis for the cell lines used.†

	D21S11	TH01	TPOX	VWA	AML	CSF1PO	D16S539	D7S820	D13S317	D5S818
HSJD-DIPG-007	29, 30	6, 9.3	8, 8	16, 17	X, Y	10, 10	13, 13	9, 12	13, 13	13, 13
QCTB-R059	29, 31.2	9	11	13, 16	X, X	12, 13	11	8, 11	12	12
OPBG-DIPG-002	29, 30	6, 6	8, 12	16, 16	X, X	11, 12	12, 12	9, 10	12, 12	10, 12

† The loci analyzed are reported, with the number of tandem repeats.

The wide use and the progressive standardization of 3D culture methods is opening new frontiers from basic to more translational research. However, more specific protocols need to be implemented in order to investigate complex 3D biological mechanisms related to the invasion of cells into matrices like Matrigel. For instance, methods describing extraction of RNA from cells cultured in Matrigel often refer to a 2D culture system with Matrigel-coated flasks or dishes [22,23]; there are few reports of RNA purification from cells completely embedded in the matrix, and these are usually without any detailed information regarding possible variations in the RNA extraction methodology.

Here we report on an RNA extraction procedure specifically adapted to purify RNA from highly invasive brain tumor primary patient-derived cells embedded into Matrigel. The previous reported 3D invasion assay [14,16] has been modified to better capture tumor heterogeneity and optimized with the aim to obtain high yield and purity of high (e.g., mRNAs) and low molecular weight RNAs (e.g., small RNAs and miRNAs) suitable for RNA sequencing analysis.

Materials & methods

Cell culture

Three primary patient-derived cell lines from patients with diffuse midline glioma H3K27M mutant (DMG-H3K27M) were used: HSJD-DIPG-007, OPBG-DIPG-002 and QCTB-R059. All the cell lines were tested for their authenticity by DNA fingerprinting (Eurofins Genomics Germany GmbH, Ebersberg, Germany) (Table 1) and verified mycoplasma free. Cells were cultured in 'Tumor Stem Media (TSM)' as previously described [24,25] and expanded as neurospheres (NSs). Once the NSs reached the diameter of 100–400 μm, they were collected and used for the invasion assay.

Invasion assay

The invasion assay performed is a modification of the method previously described [16] and adapted to 24-well plates. See protocol in the Supplementary data for detailed procedure.

Immunofluorescence

Immunofluorescence was performed on cells invading into Matrigel from individual NSs (assay performed in 96-well plates; Corning, NY, USA). The invasions were fixed with precooled 4% paraformaldehyde in phosphate -buffered saline (PBS) overnight, then washed in PBS. Cells embedded into Matrigel were transferred from the 96-well plate to an Eppendorf tube, washed twice with 1% Triton™ X-100 in Immuno-Fluorescence Fetal Calf serum solution (IFF) (1% bovine serum albumin, 2% fetal calf serum in PBS), permeabilized with 1% Triton X-100 in PBS for 45 min, then blocked for 1 h in 10% normal goat serum, 1% bovine serum albumin, 1% Triton X-100 in PBS. Cells embedded into Matrigel were then incubated overnight at 4°C with phalloidin conjugated to tetramethylrhodamine (Invitrogen, CA, USA), 1:100 in IFF. Cell nuclei were counterstained with Hoechst 1:1000 in PBS for 15 min. Images were taken using a confocal microscope (Leica TCS-SP8X laser-scanning, Leica Microsystems, Wetzlar, Germany).

RNA extraction & measurement of purity, integrity & concentration

Plates were incubated at 4°C for 45 min to let the matrix melt prior to starting RNA extraction. The protocols tested included two different ratios of matrix:TRIzol™ (TRIzol Reagent; Life Technologies, MA, USA), 1:1 and 1:3, for matrix dissociation and cell lysis. Purification of RNA was performed via centrifugation or in column. For column purification two different commercial kits were compared: Direct-Zol RNA Isolation Kit (Zymo Research, CA, USA) and ReliaPrep miRNA Cell and Tissue Miniprep System (Promega, WI, USA). Both kits include DNase treatment, but with different procedures: off-column and on-column, respectively.

Each RNA samples was checked for purity and yield on the NanoDrop™ (ThermoFisher Scientific, MA, USA). RNA concentration and integrity were measured on the 2100 Bioanalyzer (Agilent Technologies, CA, USA) using the Total RNA 6000 Nano Kit (v. II, Agilent). Measurements were performed according to the manufacturer's instructions. Electropherograms were analyzed using the Agilent 2100 Expert B.02.06 software. Table 2 summarizes the protocols tested with the reagents used in each critical step of the extraction process.

Real-time PCR

An amount of 300 ng total RNA was reverse transcribed using SuperScript™ III Reverse Transcriptase (ThermoFisher) according to the manufacturer's instructions. Reactions were performed incubating samples for 30 min at 16°C, 30 min at 42°C, 5 min at 85°C and finally cooling on ice. SensiMix II Probe Kit (Bioline, Inc., TN, USA) was used to quantify the cDNA on a QuantStudio™ 12K Flex

Table 2. List and details of all tested protocols.

Protocol index	Matrix disaggregation and cell lysis	Precipitation	Purification	DNase treatment	Cleaning
A	TRIzol ratio TRIzol:Matrigel/medium 1:1	Isopropanol	Centrifugation and supernatant removal	No	Wash in ethanol
B	TRIzol ratio TRIzol:Matrigel/medium 1:1	Ethanol 95–100%	One extraction only: column (Direct-Zol Kit)	No	Prewash buffer (×1) Wash buffer (X1)
C	TRIzol ratio TRIzol:Matrigel/medium 1:1	Ethanol 95–100%	One extraction only: column (Direct-Zol Kit)	Yes, in column	Prewash buffer (×1) Wash buffer (×1)
D	TRIzol ratio TRIzol:Matrigel/medium 3:1	Ethanol 95–100%	One extraction only: column (Direct-Zol Kit)	Yes, in column	Prewash buffer (×1) Wash buffer (×1)
E	TRIzol ratio TRIzol:Matrigel/medium 3:1	First extraction: isopropanol Second extraction: ethanol 95%	First extraction: column Second extraction: column (ReliaPrep Kit)	Yes, after the first elution	First extraction: wash buffer (×2) Second extraction: wash buffer (×2)
F	Promega lysis buffer	First extraction: isopropanol Second extraction: ethanol 95%	First extraction: column Second extraction: column (ReliaPrep Kit)	Yes, after the first elution	First extraction: wash buffer (×2) Second extraction: wash buffer (×2)

OpenArray® (Applied Biosystems, CA, USA). For the small RNAs, the evaluation of recovery efficiency between different extraction procedures was assessed by real-time PCR (TaqMan®, Applied Biosystems) using two miRNAs (hsa-miR-146a and hsa-miR-99a) and a control (U6), as previously described [26]. For detection of mRNA, primers for *ACTB* (Hs.PT.39a.22214847), *HDAC7* (Hs.PT.58.4551980), *IL6* (Hs.PT.49a.20968536) and *GUSB* (Hs.PT.39a.22214857) were purchased from Integrated DNA Technologies (PrimeTime Predesigned qPCR Assay, IA, USA) and used at a final concentration of 500 nM as per manufacturer's instructions. The qPCR cycling conditions were as follows: 95°C for 10 min, followed by 40 cycles at 95°C for 15 s and 60°C for 1 min. Data were analyzed using the SDS software (Applied Biosystems).

Results & discussion

3D tumor spheroid invasion assay

In order to extract RNA from cells invading into Matrigel, of good quality and quantity suitable for sequencing analysis, we first needed to optimize a previously reported invasion assay [14,16].

The invasion assay previously developed by Vinci *et al.* is a simple microplate method based on uniform self-assembling 3D tumor spheroids. A single spheroid, positioned at the center of the well and embedded in Matrigel, undergoes spontaneous invasion with the cancer cells evading from the NS and invading into the matrix (Figure 1A). This method, performed in 96-well plate format, has been shown to be optimal for high-content studies such as evaluating differences in cancer cell invasion modalities, quantifying the invaded area or investigating drug response effects [14,16,27], but would not be suitable for our purposes. In fact, we modified this assay to be performed in a 24-well plate format in order to increase the number of NSs by well, which would ensure a higher yield of RNA. Moreover, having more and differently sized NSs per well would also allow better capture of intratumoral heterogeneity, characteristic of many tumor types and a crucial feature of pediatric high-grade gliomas (pHGGs) [20,24,28–33]. Compared with 6- or 12-well plates, using the 24-well plates would require less reagents for the RNA extraction and thus would lower the cost of the experiments.

A pool of 30–60 NS of variable dimensions (100–400 μm diameter) was resuspended into a Matrigel/medium mixture (see protocol in Supplementary data) and dispensed in the wells. At time 0, the NSs embedded into Matrigel were imaged to assess whether they were evenly distributed into the matrix (Figure 1C, left panel).

A common feature of pHGG, critical to the clinical outcome of the patients, is the tendency of these cells to massively invade into the surrounding cerebral tissue [34,35]. This feature was well reproduced in our invasion assay, as cells started to protrude from the NS a few hours after the onset of the assay, with invasion clearly visible after 2–3 days. By day 6 the NS were not visible anymore as cells were fully dispersed into the matrix (Figure 1C). It must be noted that, although a lower plate format may be used, like 48- or 96-well plates, those wells may be too small to allow recovery of enough RNA, for example from slow-growing/poorly invasive cell lines.

Matrigel can affect the quality of the RNA extracted from embedded cells

RNA sequencing techniques require a significant amount of RNA, usually not less than 500 ng, for ordinary techniques, and it must be of high purity and integrity, with the 260/280 and 260/230 ratios between 1.8 and 2.2 and the RNA integrity number (RIN) above 8.

Methods that report on RNA extraction from cells embedded into matrix usually include an initial step of matrix disaggregation and cells–matrix separation, followed by common RNA extraction techniques such as with a TRIzol-based method or with commercial kits [20,21,33,36,37]. The matrix disaggregation can be enzymatic (proteinase K, collagenase, dispase) [37] or nonenzymatic (cell

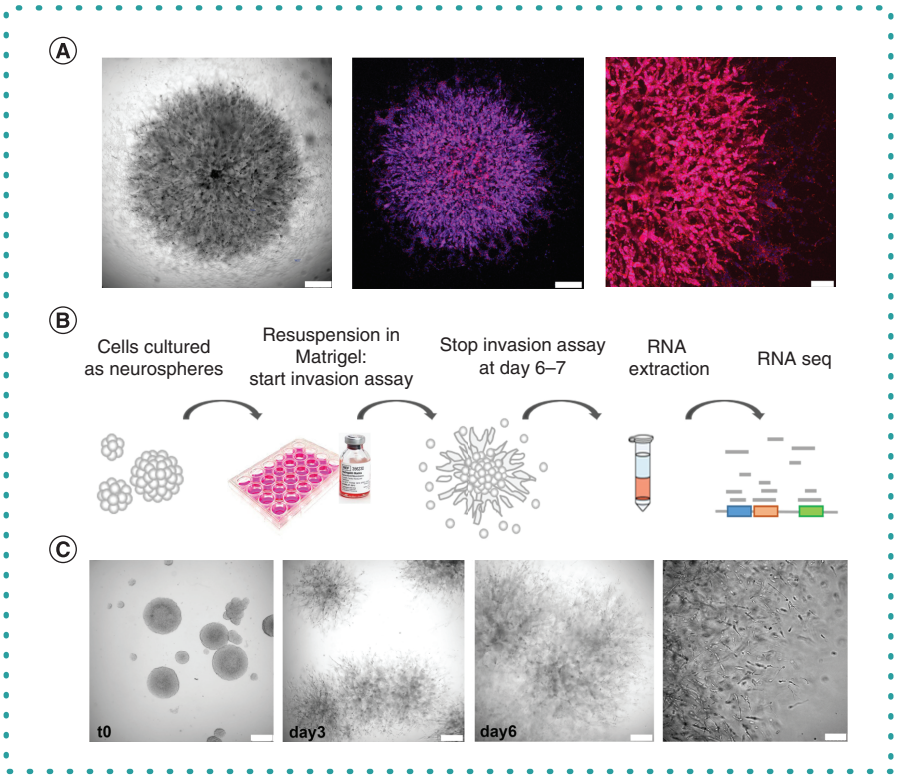

Figure 1. Pediatric high-grade glioma 3D invasion assay into Matrigel. **(A)** pHGG patient primary-derived cells (HSJD-DIPG-007) invading into Matrigel: representative bright-field image and immunofluorescent images for f-actin (red). Hoechst used for nuclei counterstain; magnification 5× left and central panel, 10× right panel. Scale bars: 250 and 100 μm, respectively. **(B)** Workflow of the method, from setting up the neurospheres to processing RNA ready for sequencing. **(C)** Representative images of pHGG patient primary-derived cells (HSJD DIPG-007) invasion into Matrigel at different time points (day 0, 3 and 6) and detail of the invasion front (day 6), showing the morphology and spatial organization of invading cells. Magnification 5× and 10×, scale bar 250 and 100 μm, respectively.
pHGG: Pediatric high-grade glioma.

recovery solution, EDTA) [20,21,33,36] and may involve an incubation step at 4°C [20,21,33,36], the temperature at which the Matrigel becomes a viscous liquid. Cell recovery is usually achieved by a centrifugation step to remove the matrix debris [20,21,33,36,37]. Augustine *et al.* reported on a series of tests for the optimization of the RNA extraction procedure, comparing different methods used to dissolve the matrix and extract the RNA. They obtained good results with the use of RLT buffer (from the Qiagen RNeasy kit) and proteinase K for matrix digestion, followed by the procedure using a column purification kit, plus DNase treatment off column [19]. Based on the data found in the literature, we decided to compare several RNA extraction methods, using different types and quantities of lysis buffer, purification techniques and including or not a DNase treatment step (Table 2).

We started with a conventional TRIzol-based RNA extraction protocol: a volume of TRIzol equal to the total volume of Matrigel/medium in each well was added for matrix degradation and cell lysis (Protocol A, Table 2). Isopropanol was then used for RNA precipitation, followed by washes in ethanol and RNA resuspension in RNase-free water. Even if the NanoDrop analysis provided optimal readouts for RNA concentration and purity, the analysis using the Bioanalyzer revealed the presence of a peak in the electropherogram profiles corresponding to low molecular weight RNA, with associated 'not applicable' RIN (Supplementary File 1). Similar profiles were obtained for the three different cell lines tested (Figure 2A & Supplementary File 1). All the samples showed an increased quantity of the small RNA fraction, representing 56.7–84.4% of the total RNA, markedly above the average of 20–30% previously reported for RNA extracted from cells [26].

To understand whether the higher percentage of small RNA found was due to the presence of Matrigel debris in the samples, we used the same protocol to extract RNA from cell pellets obtained from NS of the corresponding cell lines cultured in the absence of Matrigel. In this case, RIN values were obtained and the electropherogram profiles did not show the high small RNA peak observed in the Matrigel samples (Figure 2B). These results suggested that either the RNA extracted from the invading cells could be affected by the presence of the Matrigel, or that the invading cells would be particularly enriched in the small RNA fraction. To verify that, we extracted RNA from a blank sample containing only the Matrigel/medium mix without cells, and confirmed that the unconventional electropherogram profile was indeed due to the Matrigel itself (Figure 3A, red line).

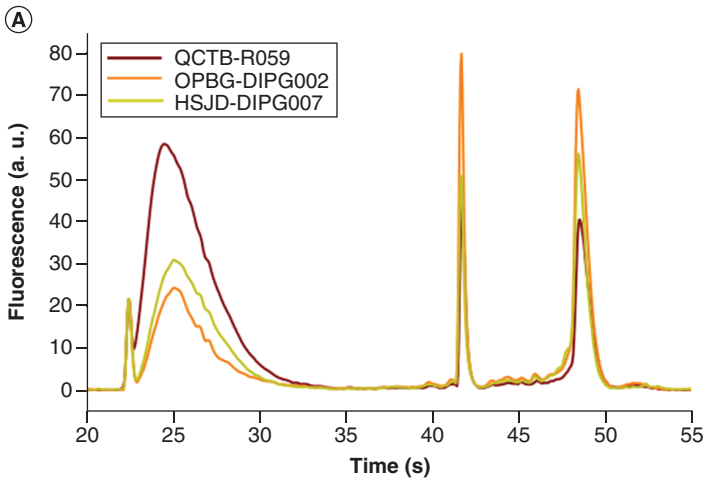

Cell line	Nanodrop RNA conc. (ng/ul)	Nanodrop 260/280 value	Nanodrop 260/230 value	Bioanalyzer RNA conc. (ng/ul)	Bioanalyzer RIN	Bioanalyzer Small RNA (%)	Volume (ul)
1. QCTB-R059	660	1.85	2.17	572	N/A	84.4	40
2. OPBG-DIPG 002	277	1.87	1.47	261	N/A	56.7	40
3. HSJD-DIPG 007	351	1.81	1.94	288	N/A	70.5	80

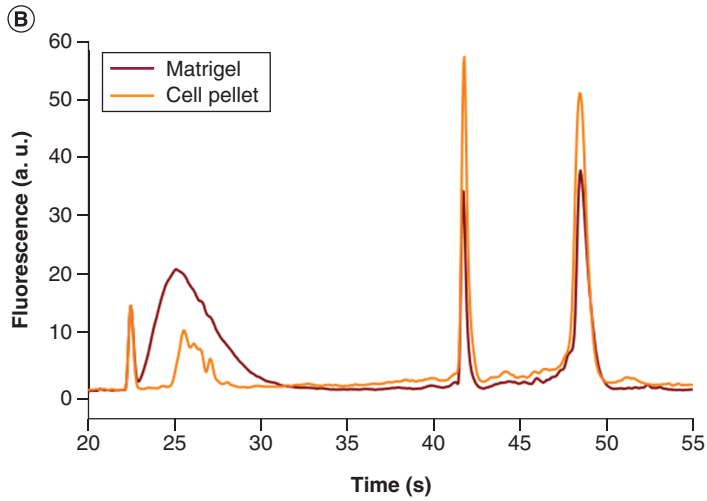

	Nanodrop RNA conc. (ng/ul)	Nanodrop 260/280 value	Nanodrop 260/230 value	Bioanalyzer RNA conc. (ng/ul)	Bioanalyzer RIN	Bioanalyzer Small RNA (%)	Volume (ul)
1. Matrigel	351	1.81	1.94	288	N/A	70.5	80
2. Cell pellet	191.2	1.80	2.41	106	9.50	20.7	30

Figure 2. RNA extraction from pediatric high-grade glioma patient primary-derived cells invading into Matrigel: Protocol A (suboptimal RNA quality). **(A)** Upper panel: Agilent 2100 Bioanalyzer electropherogram profiles of total RNA extracted from three pHGG patient-derived cell lines (QCTB-R059, OPBG-DIPG-002, HSJD-DIPG-007) invading into Matrigel following Protocol A. The profiles show the presence in all the samples of peaks in the region of the electropherogram corresponding to the small RNAs (small arrows). The area of the curve is proportional to the concentration of each sample. Lower panel: corresponding values of RNA concentration and purity measured on the Nanodrop spectrophotometer and on the Agilent 2100 Bioanalyzer. Each value is referred to RNA extracted from cells in a single well of a 24-well plate. **(B)** Upper panel: Agilent 2100 Bioanalyzer electropherograms showing direct comparison of the RNA extracted from the same cell line (HSJD-DIPG-007) grown as neurospheres and pelleted from suspension in medium or embedded in Matrigel. Lower panel: corresponding values of RNA concentration and purity obtained as described above. pHGG: Pediatric high-grade glioma.

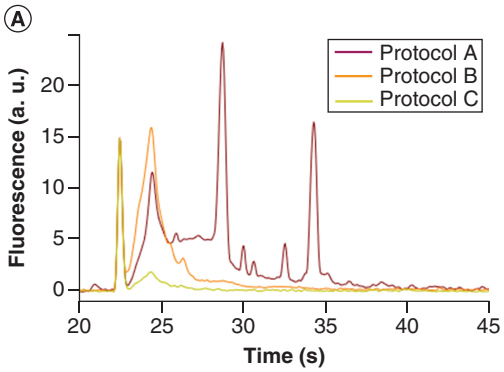

	Nanodrop			Bioanalyzer			
	RNA conc. (ng/ul)	260/280 value	260/230 value	RNA conc. (ng/ul)	RIN	Small RNA (%)	Volume (ul)
1. Protocol A	75.4	1.68	2.31	82	2.6	Not calculated	20
2. Protocol B	94.4	1.73	1.28	71	2.6	Not calculated	50
3. Protocol C	27.2	1.57	0.69	7	N/A	Not calculated	50

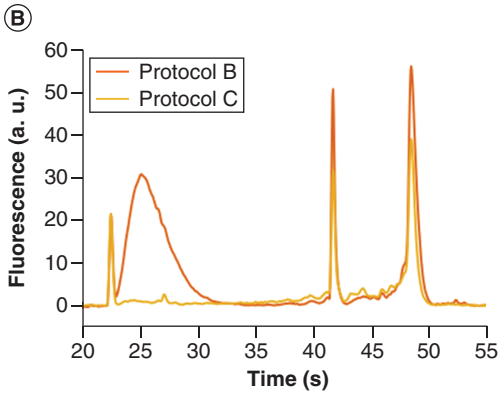

	Nanodrop			Bioanalyzer			
	RNA conc. (ng/ul)	260/280 value	260/230 value	RNA conc. (ng/ul)	RIN	Small RNA (%)	Volume (ul)
1. Protocol B	412.5	1.84	2.13	376	N/A	72.2	50
2. Protocol C	104.7	1.81	1.18	84	9.2	9.5	50

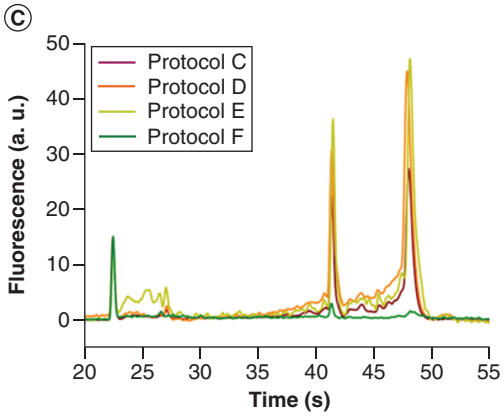

	Nanodrop			Bioanalyzer			
Sample	RNA conc. (ng/ul)	260/280 value	260/230 value	RNA conc. (ng/ul)	RIN	Small RNA (%)	Volume (ul)
1. Protocol C	104.7	1.81	1.18	84	9.2	9.5	50
2. Protocol D	122.3	1.88	1.33	164	9.4	4.9	50
3. Protocol E	106.8	2.06	1.98	181	9.7	13.8	30
4. Protocol F	10.5	1.93	0.53	15	N/A	–	30

Figure 3. RNA extraction: comparison and optimization of different protocols. **(A)** Comparison of protocols A, B and C for blank sample (only Matrigel and medium). **(B)** Comparison of protocols B and C for invading pHGG cells (HSJD-DIPG-007 cell line). **(C)** Comparison of protocols C, D, E and F for invading pHGG cells (HSJD-DIPG-007 cell line). Electropherogram profiles and corresponding values from NanoDrop and bioanalyzer readings are shown for all conditions. Each result refers to RNA extracted from one half of a well of a 24-well plate.
pHGG: Pediatric high-grade glioma.

Optimization of the RNA extraction method for invading cells embedded in Matrigel

Matrigel, which is prepared from the Engelbreth–Holm–Swarm mouse sarcoma, is known to contain traces of RNA but also DNA. This could explain the electropherogram profiles we have obtained.

To test this, we decided to use a commercially available RNA extraction kit that included a DNase digestion step (Direct-Zol, Zymo Research). Blank samples as well as invading cell samples were processed in parallel with (Protocol C) or without (Protocol B) DNase (Table 2 & Figure 3A & B). Upon treatment with DNase, the peaks that had previously been present on the electropherograms, corresponding to the low molecular weight nucleic acids, disappeared, although this was associated with a significant decrease in the concentration of the total nucleic acids, as shown from reads using both the Nanodrop and the Bioanalyzer. The purity and integrity of the RNA obtained from the invading cells treated with DNAse were of good quality, and its concentration was acceptable (Figure 3A & B).

In order to increase RNA purity and amount of the cell-specific low molecular weight RNAs, we tested additional protocols.

First, we increased the Matrigel/medium:TRIzol ratio to 1:3 (Protocol D) compared with the 1:1 ratio used in the standard protocol (Protocol C) (Figure 3C). Both protocols were followed by an RNA purification step on column and DNase treatment as described in the Direct-Zol kit manufacturer's instructions. As shown in Figure 3C, higher RNA purity and concentration were achieved with the 1:3 ratio (Protocol D).

Second, we decided to compare the RNA purification step of the Direct-Zol kit that we used in Protocol D with that of the ReliaPrep miRNA Cell and Tissue miniprep system kit, which is specifically designed to extract RNA from cells embedded into Matrigel. Both kits use columns for the RNA purification step, but ReliaPrep includes additional steps compared with the Direct-Zol kit. Moreover, the DNAse treatment is different and directly included on the RNA purification column with the Direct-Zol kit (Protocol D), while it is performed separately, after washes and elution of the RNA, with the ReliaPrep kit. The combination of the procedures for matrix digestion and cell lysis (ratio 3:1, TRIzol:matrigel/medium) with purification in column and DNAse treatment (ReliaPrep kit) are identified as Protocol E. When we compared the RNA purification steps of the two kits after our 1:3 matix:TRIzol ratio (Figure 3C), we could observe that protocols D and E both provided a good concentration and integrity of the RNA. However, we had a better RNA recovery with Protocol D, while the RNA purity was better following Protocol E (see Nanodrop values; Figure 3C & Supplementary File 1). Also, Protocol E allows the recovery of a higher percentage of small RNA species compared with Protocol D (Figure 3C & Supplementary File 1). For both procedures, the RINs were variable but above 8 (Figure 3C & Supplementary File 1).

Finally, we tested the ReliaPrep kit following the instructions recommended by the manufacturer (Protocol F). This kit uses a cell lysis buffer composed of guanine thiocyanate plus 1-thioglycerol, but without phenol, and thus is different from the TRIzol. This protocol gave us the worst results in terms of RNA yield, mainly due to column occlusion and eluate retention (Figure 3C, red line).

mRNA & miRNA levels in RNA samples prepared following protocols A, E & F

Protocol E gave us the best results in terms of purity, integrity and yield of the total RNA extracted from cells invading into the Matrigel. In addition, this protocol allowed the recovery of low molecular weight RNAs.

To further check on the nature of the different types of RNAs contained in our samples, as well as on the efficiency of our protocol in recovering cell-specific RNAs, we performed real-time PCR analysis.

For this, we selected two mRNAs, *IL6* and *HDAC7*, and two low molecular weight RNAs, miRNA-99A and miRNA-146a, which we identified as being expressed at different levels in pHGG invading cells in preliminary RNAseq data analysis (Ferretti *et al*., unpublished data). The two selected miRNAs are found in mouse and human with a highly conserved sequence; therefore the qPCR probes are not selective for one or the other species but they could be useful to detect eventually the presence of any residual RNA of Matrigel mouse origin in the samples. Thus for the qPCR we considered RNA extracted from HSJD-DIPG-007 invading cells into the Matrigel and blank samples (RNA extraction performed from Matrigel/medium only).

We compared RNA samples extracted following Protocol A (our initial method), Protocol E (our elective method) and Protocol F (using the ReliaPrep kit only).

The real-time PCR revealed no difference in the mRNA levels of *HDAC7* between the RNA samples from the invading cells prepared with the three protocols. The *IL6* mRNA was expressed at a lower level compared with *HDAC7* using Protocols A and E, but no expression was detected with Protocol F (Figure 4). For both mRNAs, no signal was detected for *HDAC7* or *IL6* in the blank samples for the three protocols, confirming the quality of our RNA preparation procedure. The results obtained for *IL6* mRNA are in line with the RNA concentration values obtained with the three protocols (Figure 3C). For genes expressed at low levels, Protocol F (ReliaPrep kit) is not ideal as the overall RNA yield is low (Figure 3C) and consequently the specific gene expression levels are also low (Figure 4).

With regard to miR-99a and miR-146a, they were both detected in all the RNA samples obtained from the invading cells but the levels were significantly higher in the RNA extracted following Protocol A. This may potentially be explained by the presence of RNA contaminants present in the Matrigel. In fact, for both miRNAs, a signal was detected in the blank sample for Protocol A, while no signal was detected using the other two protocols (Figure 4).

The study presents some limitations, both technical and biological. From a technical point of view, a minimum number of 30–60 NSs per well in a 24-well plate format must be used in order to recover an amount of RNA sufficient for standard RNA sequencing methods. This may be particularly important for slow-growing/poorly invasive cells. In comparison to our method, a lower quantity of RNA may be used for low-input and ultra-low-input RNA sequencing protocols. However, those are generally more expensive compared with standard sequencing methods. The method we present is intended for a wider application and to be most accessible to all laboratories (i.e., not low-input and ultra low-input protocols). From a biological point of view, a limitation could be represented by the heterogeneous size of the NSs used for the assay and the different biological processes involved: stem cell features in smaller spheres, hypoxia-driven invasion in larger spheres. As mentioned above, though, this heterogeneity may more faithfully reflect some physiological features of invasive tumors *in vivo*.

In conclusion, we optimized an RNA extraction protocol (Protocol E) for primary pHGG cells invading into Matrigel. Our procedure is relevant for studying different types of RNA molecules, including both high and low molecular weight RNAs [26]. Our main goal was to obtain RNA of good quality (purity and integrity) and high yield for subsequent RNA sequencing analysis. The optimized protocol has

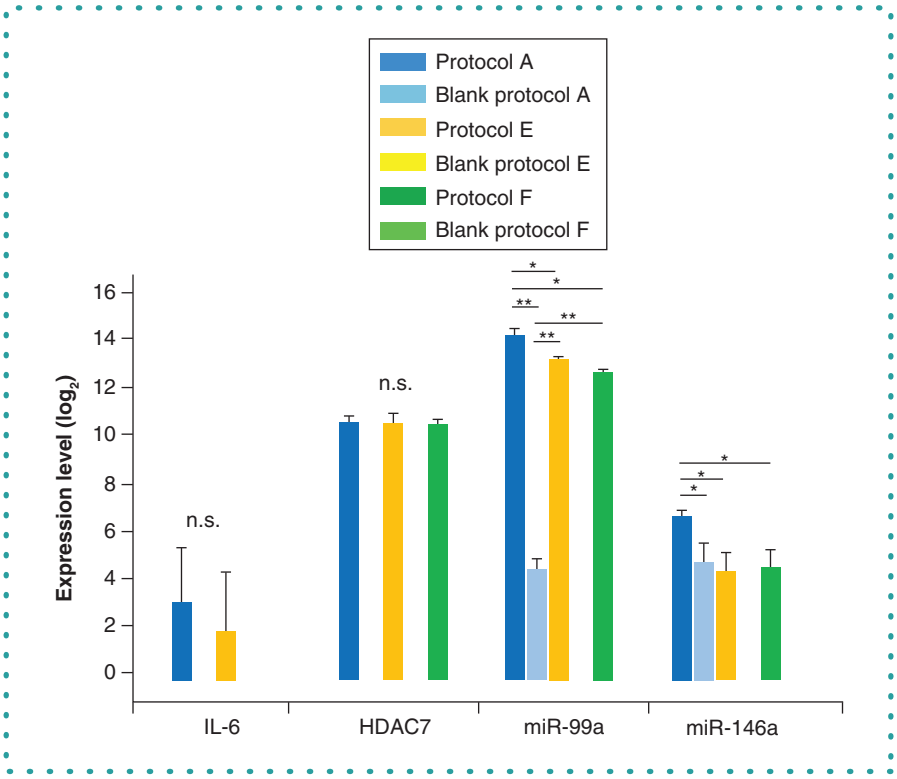

Figure 4. Validation by real-time PCR of type and quality of RNA extracted. Real-time PCR assay of RNA obtained from cells invading into Matrigel extracted with Protocol A (blue bar), the elective Protocol E (orange bar) and Protocol F (green bar). For each protocol the blank samples (RNA extracted from Matrigel/medium, no cells) were also considered (light blue, yellow and light green bars, respectively). 5 ng of total RNA was used for all samples. HSJD-DIPG-007 cells were used. Gene names and miRNA are reported.
Statistical analysis was performed by using one-way analysis of variance. For qPCR, statistical analyses were performed by using the 2-ΔΔCt method. Quantitative data are presented as mean ± standard deviation. All experiments were performed in duplicate. Differences were considered significant at *$p < 0.05$; **$p < 0.01$.

proven to be useful for our ongoing studies on pHGG primary-derived cell lines and may be applicable to study the gene expression of different highly invasive cell lines from other tumor types assayed in similar culture conditions.

Supplementary data

To view the supplementary data that accompany this paper please visit the journal website at: www.future-science.com/doi/suppl/10.2144/btn-2021-0001

Author contributions

Concept and design: R Ferretti, A Masotti and M Vinci. Experiments and data collection: R Ferretti, A Baldassarre. Data analysis and interpretation: R Ferretti, A Baldassarre, A Masotti. Reagents, samples, cell lines: A Carcaboso, A Moore, A Carai, A Mastronuzzi. Funding acquisition: M Vinci, R Ferretti, E de Billy and M Vinci drafted and wrote the manuscript; all authors reviewed and approved the final manuscript.

Financial & competing interests disclosure

This study was supported by Children with Cancer UK grant (16-234) and The Italian Ministry of Health Ricerca Corrente. M Vinci is a Children with Cancer UK Fellow. R Ferretti is a recipient of Fondazione Veronesi Fellowship (2018 and 2019). The authors also acknowledge Fondazione Heal for their support. The authors have no other relevant affiliations or financial involvement with any organization or entity with a financial interest in or financial conflict with the subject matter or materials discussed in the manuscript apart from those disclosed.

No writing assistance was used for this manuscript.

Ethical conduct of research

The authors state that they have obtained appropriate institutional review board approval or have followed the principles outlined in the Declaration of Helsinki for all human or animal experimental investigations. In addition, for investigations involving human subjects, informed consent has been obtained from the participants involved.

Open access

References

Papers of special note have been highlighted as: • of interest

1. Brancato V, Oliveira JM, Correlo VM, Reis RL, Kundu SC. Could 3D models of cancer enhance drug screening? *Biomaterials* 232, 119744 (2020).
2. Jia W, Jiang X, Liu W *et al.* Effects of three-dimensional collagen scaffolds on the expression profiles and biological functions of glioma cells. *Int. J. Oncol.* 52(6), 1787–1800 (2018).
3. Tibbitt MW, Anseth KS. Hydrogels as extracellular matrix mimics for 3D cell culture. *Biotechnol. Bioeng.* 103(4), 655–663 (2009).
4. Wilson TJ, Zamler DB, Doherty R, Castro MG, Lowenstein PR. Reversibility of glioma stem cells' phenotypes explains their complex *in vitro* and *in vivo* behavior: discovery of a novel neurosphere-specific enzyme, cGMP-dependent protein kinase 1, using the genomic landscape of human glioma stem cells as a discovery tool. *Oncotarget* 7(39), 63020–63041 (2016).
5. Caliari SR, Burdick JA. A practical guide to hydrogels for cell culture. *Nat. Methods* 13(5), 405–414 (2016).
6. Koh I, Cha J, Park J, Choi J, Kang SG, Kim P. The mode and dynamics of glioblastoma cell invasion into a decellularized tissue-derived extracellular matrix-based three-dimensional tumor model. *Sci. Rep.* 8(1), 4608 (2018).

• **Discusses the need for more appropriate recapitulation of the glioblastoma tumor microenvironment, including biochemical and biophysical elements, in 3D *in vitro* experiments.**

7. Hoque J, Sangaj N, Varghese S. Stimuli-responsive supramolecular hydrogels and their applications in regenerative medicine. *Macromol. Biosci.* 19(1), e1800259 (2019).
8. Quereda V, Hou S, Madoux F, Scampavia L, Spicer TP, Duckett D. A cytotoxic three-dimensional-spheroid, high-throughput assay using patient-derived glioma stem cells. *SLAS Discov.* 23(8), 842–849 (2018).
9. Drost J, Clevers H. Organoids in cancer research. *Nat Rev Cancer* 18(7), 407–418 (2018).
10. Goers L, Freemont P, Polizzi KM. Co-culture systems and technologies: taking synthetic biology to the next level. *J. R. Soc. Interface* 11(96), 20140065 (2014).
11. Hutmacher DW. Biomaterials offer cancer research the third dimension. *Nat. Mater.* 9(2), 90–93 (2010).
12. Nath S, Devi GR. Three-dimensional culture systems in cancer research: focus on tumor spheroid model. *Pharmacol. Ther.* 163, 94–108 (2016).
13. Simunovic M, Brivanlou AH. Embryoids, organoids and gastruloids: new approaches to understanding embryogenesis. *Development* 144(6), 976–985 (2017).
14. Vinci M, Gowan S, Boxall F *et al.* Advances in establishment and analysis of three-dimensional tumor spheroid-based functional assays for target validation and drug evaluation. *BMC Biol.* 10, 29 (2012).
15. Jaganathan H, Gage J, Leonard F *et al.* Three-dimensional *in vitro* co-culture model of breast tumor using magnetic levitation. *Sci. Rep.* 4, 6468 (2014).
16. Vinci M, Box C, Eccles SA. Three-dimensional (3D) tumor spheroid invasion assay. *J. Vis. Exp.* (99), e52686 (2015).
17. Chen JWE, Pedron S, Harley BaC. The combined influence of hydrogel stiffness and matrix-bound hyaluronic acid content on glioblastoma invasion. *Macromol. Biosci.* 17(8), 10.1002/mabi.201700018 (2017).

• **Shows how the composition and the physical properties of the extracellular matrix can affect glioblastoma invasion.**

18. Geckil H, Xu F, Zhang XH, Moon S, Demirci U. Engineering hydrogels as extracellular matrix mimics. *Nanomedicine (Lond.)* 5(3), 469–484 (2010).
19. Augustine TN, Dix-Peek T, Duarte R, Candy GP. Establishment of a heterotypic 3D culture system to evaluate the interaction of TREG lymphocytes and NK cells with breast cancer. *J. Immunol. Methods* 426, 1–13 (2015).

• **Discusses the lack of suitable methods for RNA extraction from cells embedded into Matrigel and addresses the problem by comparing a number of them.**

20. Dwyer AR, Ellies LG, Holme AL, Pixley FJ. A three-dimensional co-culture system to investigate macrophage-dependent tumor cell invasion. *J. Biol. Methods* 3(3), e49 (2016).
21. Lee GY, Kenny PA, Lee EH, Bissell MJ. Three-dimensional culture models of normal and malignant breast epithelial cells. *Nat. Methods* 4(4), 359–365 (2007).
22. Laragione T, Brenner M, Li W, Gulko PS. Cia5d regulates a new fibroblast-like synoviocyte invasion-associated gene expression signature. *Arthritis Res. Ther.* 10(4), R92 (2008).
23. Olsen CL, Hsu PP, Glienke J, Rubanyi GM, Brooks AR. Hedgehog-interacting protein is highly expressed in endothelial cells but down-regulated during angiogenesis and in several human tumors. *BMC Cancer* 4, 43 (2004).
24. Pericoli G, Petrini S, Giorda E *et al.* Integration of multiple platforms for the analysis of multifluorescent marking technology applied to pediatric GBM and DIPG. *Int. J. Mol. Sci.* 21(18), 6763 92020).
25. Vinci M, Burford A, Molinari V *et al.* Functional diversity and cooperativity between subclonal populations of pediatric glioblastoma and diffuse intrinsic pontine glioma cells. *Nat. Med.* 24(8), 1204–1215 (2018).
26. Masotti A, Caputo V, Da Sacco L, Pizzuti A, Dallapiccola B, Bottazzo GF. Quantification of small non-coding RNAs allows an accurate comparison of miRNA expression profiles. *J. Biomed. Biotechnol.* 2009, 659028 (2009).

• **Relevant for low-molecular-weight RNAs quantification and expression profiles.**

27. Gudbergsson JM, Kostrikov S, Johnsen KB *et al.* A tumorsphere model of glioblastoma multiforme with intratumoral heterogeneity for quantitative analysis of cellular migration and drug response. *Exp. Cell Res.* 379(1), 73–82 (2019).
28. Hoffman LM, Dewire M, Ryall S *et al.* Spatial genomic heterogeneity in diffuse intrinsic pontine and midline high-grade glioma: implications for diagnostic biopsy and targeted therapeutics. *Acta Neuropathol. Commun.* 4, 1 (2016).
29. Januskeviciene I, Petrikaite V. Heterogeneity of breast cancer: the importance of interaction between different tumor cell populations. *Life Sci.* 239, 117009 (2019).
30. Patel AP, Tirosh I, Trombetta JJ *et al.* Single-cell RNA-seq highlights intratumoral heterogeneity in primary glioblastoma. *Science* 344(6190), 1396–1401 (2014).
31. Sasaki N, Clevers H. Studying cellular heterogeneity and drug sensitivity in colorectal cancer using organoid technology. *Curr. Opin. Genet. Dev.* 52, 117–122 (2018).
32. Tabassum DP, Polyak K. Tumorigenesis: it takes a village. *Nat. Rev. Cancer* 15(8), 473–483 (2015).
33. Ampuja M, Jokimaki R, Juuti-Uusitalo K, Rodriguez-Martinez A, Alarmo EL, Kallioniemi A. BMP4 inhibits the proliferation of breast cancer cells and induces an MMP-dependent migratory phenotype in MDA-MB-231 cells in 3D environment. *BMC Cancer* 13, 429 (2013).
34. Caretti V, Bugiani M, Freret M *et al.* Subventricular spread of diffuse intrinsic pontine glioma. *Acta Neuropathol.* 128(4), 605–607 (2014).
35. Mair DB, Ames HM, Li R. Mechanisms of invasion and motility of high-grade gliomas in the brain. *Mol. Biol. Cell* 29(21), 2509–2515 (2018).
36. Elamin E, Jonkers D, Juuti-Uusitalo K *et al.* Effects of ethanol and acetaldehyde on tight junction integrity: *in vitro* study in a three dimensional intestinal epithelial cell culture model. *PLoS ONE* 7(4), e35008 (2012).
37. Osiecka-Iwan A, Hyc A, Niderla-Bielinska J, Moskalewski S. Chondrocyte-associated antigen and matrix components in a 2- and 3-dimensional culture of rat chondrocytes. *Mol. Med. Rep.* 1(6), 881–887 (2008).